ChemComm

COMMUNICATION

View Article Online
View Journal | View Issue

Cite this: *Chem. Commun.*, 2024, **60**, 4366

Received 18th January 2024,
Accepted 22nd February 2024

DOI: 10.1039/d4cc00272e

rsc.li/chemcomm

BODIPY phototether enables oligonucleotide cyclization and subsequent deprotection by tissue-transparent red light†

Lucie Wohlrábová, [ab] Marlen Sahlbach,[c] Alexander Heckel [c] and Tomáš Slanina *[a]

***meso*-methyl-BODIPY photocages release a leaving group upon visible light irradiation but often lack thermal stability. In turn, our thermally-stable, red-shifted BODIPY phototether allows oligonucleotide cyclization, preventing complementary strand hybridization. Hybridization resumes upon red-NIR irradiation, disconnecting the phototether by oxidative cleavage, which is easily monitored by a blue shift in fluorescence.**

Oligonucleotides are short nucleic acids that hybridize to a complementary sequence, with various biological functions.[1] Access to oligonucleotides by solid phase synthesis has prompted the development of many biological and medical diagnostic technologies.[2] Moreover, oligonucleotides can be designed to target specific genes and are, as such, promising candidates for targeted therapy.[3,4] Native oligonucleotides, however, show low stability and are degraded by nucleases limiting their applications. This problem can be overcome by protecting oligonucleotides against decomposition, including through cyclization.

Cyclization of oligonucleotides blocks their ability to hybridize with a complementary strand and, therefore, masks their function. In fact, transient cyclization with subsequent release is an efficient strategy of gene regulation.[5] This process can be controlled using a photoactivatable tether (phototether)[6] to temporarily connect two segments of oligonucleotides and subsequently release them by light in a defined time, space, and concentration.[5]

Despite their potential, photocage applications as phototethers are still incipient because phototethers must absorb in the tissue-transparent window and have low toxicity and defined photoreactivity while remaining thermally stable under cyclization conditions. Only a few photocages, such as cyanine[7,8] and anthracene,[9] have been introduced so far, though with limited stability and absorption properties.[10] To meet these requirements, BODIPY photocages stand out as promising alternatives.

BODIPY photocages can be readily synthesized and derivatized,[11] displaying multimodal photoreactivity.[12] Furthermore, their spectral properties change upon irradiation, which enables photorelease monitoring.[13] However, the biological use of the most common *meso*-methyl substituted BODIPY photocages is limited by the low thermal stability of their C-heteroatom bond, suffering from hydrolysis and reductive homolytic cleavage.[13,14] Therefore, we hypothesized that a more stable, *meso*-phenyl π-extended BODIPY phototether could be designed to be cleaved by the recently described photooxidative styryl cleavage induced by singlet oxygen.[13,15,16]

In this study, we aimed at developing a BODIPY phototether used for oligonucleotide cyclization and subsequent cleavage by red light. As a result of photoxidizing one of the styryl moieties, irradiation shortened the conjugated π-system, resulting in a blue shift in absorption and emission monitored by multichannel fluorescence.[13] Photocleavage of cyclized oligonucleotides should not affect the biological environment because the singlet oxygen produced by the excited state fluorophore is consumed in this process. A 15-mer DNA oligonucleotide was cyclized and subsequently photoreleased, showing marked changes in hybridization with a complementary strand in melting point measurements, thereby demonstrating the potential applicability of this concept.

We synthesized phototether **1** (Scheme 1) by a Knoevenagel condensation of an azide-containing aromatic aldehyde and *meso*-phenyl-substituted BODIPY. The synthesis started from 4-(2-hydroxyethoxy)benzaldehyde **2**, which was treated with PPh_3I_2 and imidazole to obtain the iodinated analogue **3**. Then, iodine was substituted with azide yielding **4**. BODIPY scaffold **5**

[a] *Institute of Organic Chemistry and Biochemistry, Flemingovo náměstí 542, Prague 160 00, Czech Republic. E-mail: tomas.slanina@uochb.cas.cz*
[b] *Department of Organic Chemistry, University of Chemistry and Technology Prague, 166 28, Prague 6, Czech Republic*
[c] *Goethe Universität Frankfurt, Max-von-Laue-Strasse 7, Frankfurt am Main 60438, Germany*

† Electronic supplementary information (ESI) available. See DOI: https://doi.org/10.1039/d4cc00272e

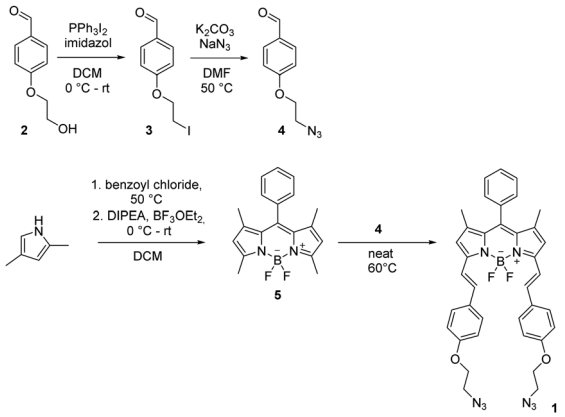

Scheme 1 Synthesis of a BODIPY phototether **1**.

was prepared by condensation of 2,4-dimethylpyrrole with benzoyl chloride and further complexation with $BF_3{\cdot}OEt_2$. Knoevenagel condensation of **5** with an excess of **4** provided phototether **1**.

Subsequently, we synthesized a model 15-mer DNA oligonucleotide: **5′ m1-GCA TAA ATA AAG GTG-m2 3′** (**A**), modified with propargyl groups at the 3' and 5' ends (*m* = alkyne modification; for details, see Supporting Information (SI)). Oligonucleotide **A** was further cyclized by BODIPY phototether **1** to **1A** *via* a copper-catalyzed azide–alkyne cycloaddition click reaction in a DMSO-water mixture (Fig. 1A). To avoid head–tail dimerization or polymerization, the oligonucleotide sequence was decorated with alkyne groups attached to both ends, whereas **1** was symmetrically decorated with two azido groups allowing cyclization *via* triazole formation. The click reaction was conducted under high dilution conditions ($c \sim 0.7$ mM), favouring the intermolecular cyclization between compound **1** and oligonucleotide **A** over intermolecular polymerization. Both **1** and **1A** were thermally stable allowing for chromatographic purification.

Due to its limited aqueous solubility, photophysical and photochemical data for **1** were measured in a MeOH:DCM mixture (9 : 1, *v*/*v*). The BODIPY phototether proved to be a strong chromophore, with excellent absorption in the red region ($\lambda_{abs,max}$ = 636 nm) and fluorescent properties (Φ_f = 0.16, Table 1). Although **1** aggregated in aqueous media (see SI for more details), it did not require any structural modification by water-solubilizing groups for oligonucleotide cyclization. Attaching **1** to **A** produced water-soluble, cyclized oligonucleotide **1A**, whose spectroscopic properties in water were comparable to those of **1**. The emission maximum of **1A** was 662 nm and hence red-shifted by 10 nm in relation to **1**.

We designed our BODIPY phototether based on photooxygenation cleavage of styryl-substituted BODIPY.[13,15,16] As in cyanine photocages, the electron-rich double bonds of **1** reacted with singlet oxygen produced by the excited dye through sensitization. This oxidative process yielded a dioxetane intermediate **1-diox**, which subsequently decomposed to two aromatic aldehydes, **1-irr** and a benzaldehyde derivative (Fig. 1B). We found **1-diox** and its oxidation products to accumulate within the irradiation time frame (Fig. S14, ESI†), which limits achieving full conversion from **1** to **1-irr**. However, in **1A** photolysis, the preference for the formation of **1A-irr** is driven by entropy, which promotes the linearization of the tethered cycle, facilitating thermal decomposition of **1A-diox** (dioxetane analogue of cyclic oligonucleotide **1A**) to **1A-irr**, thereby cleaving the cyclized oligonucleotide (Fig. 1C). Because the molar masses of **1A-diox** and **1A-irr** are identical, the photocleavage of **1A** cannot be studied by mass spectrometry. Therefore, the oligonucleotide recovery was validated through spectroscopy and melting point measurements (*vide infra*).

Irradiation of **1** was followed by UV/vis and fluorescence spectroscopy (Fig. 2A). The absorption and emission maxima of the photoproduct were significantly hypsochromically shifted (572 nm and 588 nm respectively). Accordingly, oligonucleotide

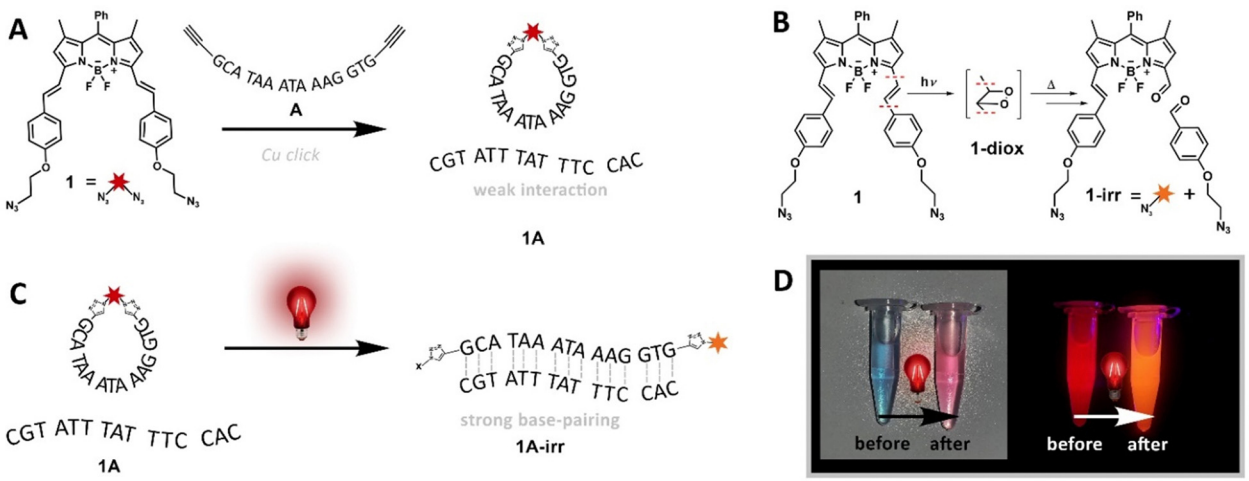

Fig. 1 (A) Oligonucleotide cyclization by a BODIPY phototether *via* a Cu^I-catalysed coupling reaction. (B) Uncaging mechanism of BODIPY phototether **1**. (C) Uncaging of cyclized oligonucleotide **1A**. (D) Left: change in the color of **1** upon irradiation; right: change in the emission of **1** upon irradiation (excited by UV light).

Table 1 Spectroscopic and photochemical properties of the studied compounds

Compd.	λ_{abs} [a]	ε_{max} [b]	λ_{em} [c]	$\Delta\tilde{\nu}$ [d]	Φ_r [e] $\times 10^{-6}$	Φ_r (O_2) [e] $\times 10^{-6}$	$\Phi_r \bullet \varepsilon_{max}$	Φ_f
1 [f]	636	138 000	652	386	0.32 ± 0.1	n.d.	0.044	0.16 ± 0.01
1A [g]	648	125 000	662	326	1.2 ± 0.1	1.5 ± 0.1	0.15	n.d. [h]
1A irr [g]	572	n.d. [h]	588	475	n.r. [i]	n.r. [i]	n.r [i]	n.d. [h]

[a] Absorption maximum in nm. [b] Molar absorption coefficient at the absorption maximum in M^{-1} cm^{-1}. [c] Fluorescence maximum in nm. [d] Stokes shift in cm^{-1}. [e] Photorelease quantum yield, Φ_r aerated and $\Phi_r(O_2)$ saturated with O_2. [f] Measured in the mixture of dichloromethane/methanol (1 : 9, v/v). [g] Measured in PBS. [h] n.d. = not determined. [i] n.r. = not relevant.

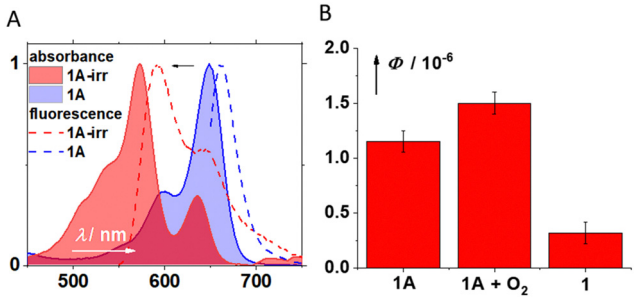

Fig. 2 (A) Normalized absorption and emission spectra of **1A** and **1A-irr** in PBS, and (B) photorelease quantum yields upon irradiation with 617 nm light.

1A photocleavage could be easily monitored by a change in the absorption and emission (Fig. 1D).

The cyclized oligonucleotide **1A** underwent photorelease in PBS with the quantum yield of 1.2×10^{-6}. Irradiating oxygen-saturated solutions of **1A** increased the photoreaction quantum yield by 1.2-fold, showing the oxygen effect. The quantum yield of **1** was ~4-fold lower than that for **1A** (Fig. 2B), most likely due to the solvent effect (different polarity, lower oxygen solubility in methanol[17] (c = 4.15 10^{-4} M) than in water[18] (c = 1.22 10^{-3} M)) and to entropy effects of cyclization. The excellent absorption properties of both **1** and **1A** compensate for the low photorelease quantum yields, resulting in acceptable uncaging cross-sections of 0.044 and 0.15, respectively (Table 1).

The photocleavage of the cyclized oligonucleotide **1A** was followed by HPLC (Fig. 3A) until quantitative deprotection.

The starting material was consumed and resulted in the formation of **1A-irr** as a main product. To demonstrate the ability to control the hybridization of **A** by light, melting points were measured after the addition of an equimolar amount of a complementary strand. While the melting points of **A** and **1A-irr** were almost identical (51.6 and 52.8 °C, respectively, Fig. 3B and C), the melting point of cyclized **1A** was not detected due to the absence of duplex formation (Fig. 3D). This finding proves that the cyclization of oligonucleotide blocked its ability to hybridize to a complementary strand and the subsequent photorelease restored this property.

We demonstrated that the BODIPY phototether enables temporary oligonucleotide cyclization and subsequent photorelease by red-NIR light. Thermally stable and easily accessible, the BODIPY phototether is activated by light in the tissue-transparent window, and its distribution and release are easily

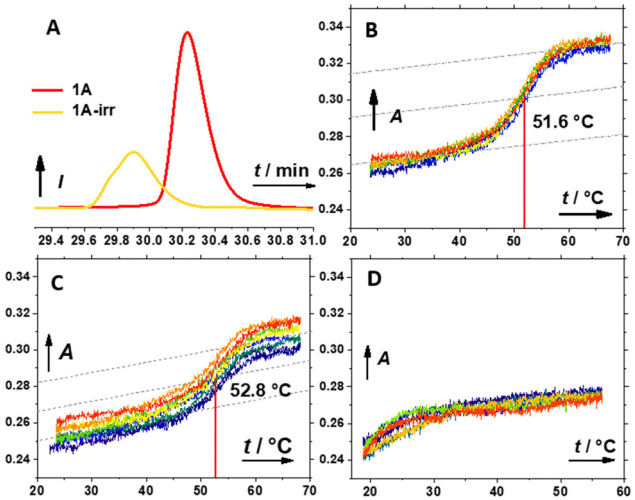

Fig. 3 (A) Zoomed-in LC-MS chromatograms extracted at 254 nm: red: starting material **1A**. Yellow: product **1A-irr**. Melting points (5–7 consecutive measurements) of (B) linear 15-mer oligonucleotide **A**, (C) uncaged oligonucleotide **1A-irr** and (D) cyclized oligonucleotide **1**.

monitored by fluorescence spectroscopy. A 15-mer DNA oligonucleotide can be temporarily cyclized, blocking its hybridization ability. This function is resumed upon irradiation with red-NIR light that cleaves the phototether with acceptable uncaging cross-sections. Photocleavage is oxygen-dependent suggesting that oxygen plays a key role in this process.

T. S., A. H. conceptualization, funding acquisition, resources, supervision A. H. software L. W. formal analysis, visualization, investigation, M. S. methodology, investigation T. S., L. W. writing – original draft, T. S., A. H. writing – review & editing.

The authors thank the Czech Science Foundation (project No. 22-20319S) for funding and Carlos V. Melo for editing the manuscript.

Conflicts of interest

There are no conflicts to declare.

References

1 R. Lakhia, A. Mishra and V. Patel, Manipulation of Renal Gene Expression Using Oligonucleotides, *Methods in Cell Biology*, Elsevier, 2019, vol. 154, pp 109–120, DOI: 10.1016/bs.mcb.2019.05.006.

2 C. F. Bennett, Therapeutic Antisense Oligonucleotides Are Coming of Age, *Annu. Rev. Med.*, 2019, **70**(1), 307–321, DOI: 10.1146/annurev-med-041217-010829.
3 L. Moumné, A.-C. Marie and N. Crouvezier, Oligonucleotide Therapeutics: From Discovery and Development to Patentability, *Pharmaceutics*, 2022, **14**(2), 260, DOI: 10.3390/pharmaceutics14020260.
4 S. Thakur, A. Sinhari, P. Jain and H. R. Jadhav, A Perspective on Oligonucleotide Therapy: Approaches to Patient Customization, *Front. Pharmacol.*, 2022, 13.
5 P. Müller, P. Seyfried, A. Frühauf and A. Heckel, Chapter Five – Phosphodiester Photo-Tethers for the (Multi-)Cyclic Conformational Caging of Oligonucleotides, In: *Methods in Enzymology*, ed. Deiters, A., *Optochemical Biology*, Academic Press, 2019, vol. 624, pp. 89–111, DOI: 10.1016/bs.mie.2019.04.019.
6 P. Seyfried, L. Eiden, N. Grebenovsky, G. Mayer and A. Heckel, Photo-Tethers for the (Multi-)Cyclic, Conformational Caging of Long Oligonucleotides, *Angew. Chem., Int. Ed.*, 2017, **56**(1), 359–363, DOI: 10.1002/anie.201610025.
7 L. Yang, H. B. Kim, J.-Y. Sul, S. B. Yeldell, J. H. Eberwine and I. J. Dmochowski, Efficient Synthesis of Light-Triggered Circular Antisense Oligonucleotides Targeting Cellular Protein Expression, *ChemBioChem*, 2018, **19**(12), 1250–1254, DOI: 10.1002/cbic.201800012.
8 P. Müller, M. Sahlbach, S. Gasper, G. Mayer, J. Müller, B. Pötzsch and A. Heckel, Controlling Coagulation in Blood with Red Light, *Angew. Chem., Int. Ed.*, 2021, **60**(41), 22441–22446, DOI: 10.1002/anie.202108468.
9 S. G. König and A. Mokhir, 'Caged' Peptide Nucleic Acids Activated by Red Light in a Singlet Oxygen Mediated Process, *Bioorg. Med. Chem. Lett.*, 2013, **23**(24), 6544–6548, DOI: 10.1016/j.bmcl.2013.11.003.
10 M. Henary and M. Mojzych, Stability and Reactivity of Polymethine Dyes in Solution, In: Heterocyclic Polymethine Dyes: Synthesis, Properties and Applications, ed. L. Strekowski, *Topics in Heterocyclic Chemistry*, Springer, Berlin, Heidelberg, 2008, pp. 221–238, DOI: 10.1007/7081_2008_111.
11 T. Slanina, P. Shrestha, E. Palao, D. Kand, J. A. Peterson, A. S. Dutton, N. Rubinstein, R. Weinstain, A. H. Winter and P. Klán, In Search of the Perfect Photocage: Structure–Reactivity Relationships in Meso-Methyl BODIPY Photoremovable Protecting Groups, *J. Am. Chem. Soc.*, 2017, **139**(42), 15168–15175, DOI: 10.1021/jacs.7b08532.
12 P. Shrestha, D. Kand, R. Weinstain and A. H. Winter, Meso-Methyl BODIPY Photocages: Mechanisms, Photochemical Properties, and Applications, *J. Am. Chem. Soc.*, 2023, **145**(32), 17497–17514, DOI: 10.1021/jacs.3c01682.
13 A. Poryvai, M. Galkin, V. Shvadchak and T. Slanina, Red-Shifted Water-Soluble BODIPY Photocages for Visualisation and Controllable Cellular Delivery of Signaling Lipids, *Angew. Chem., Int. Ed.*, 2022, **61**(34), e202205855, DOI: 10.1002/anie.202205855.
14 L. Wohlrábová, J. Okoročenkova, E. Palao, E. Kužmová, K. Chalupský, P. Klán and T. Slanina, Sulfonothioated Meso-Methyl BODIPY Shows Enhanced Uncaging Efficiency and Releases H2Sn, *Org. Lett.*, 2023, **25**(36), 6705–6709.
15 J. A. Peterson, C. Wijesooriya, E. J. Gehrmann, K. M. Mahoney, P. P. Goswami, T. R. Albright, A. Syed, A. S. Dutton, E. A. Smith and A. H. Winter, Family of BODIPY Photocages Cleaved by Single Photons of Visible/Near-Infrared Light, *J. Am. Chem. Soc.*, 2018, **140**(23), 7343–7346, DOI: 10.1021/jacs.8b04040.
16 Y. Xu, S. Lin, R. He, Y. Zhang, Q. Gao, D. K. P. Ng and J. Geng, C═C Bond Oxidative Cleavage of BODIPY Photocages by Visible Light, *Chem. – Eur. J.*, 2021, **27**(44), 11268–11272, DOI: 10.1002/chem.202101833.
17 T. Sato, Y. Hamada, M. Sumikawa, S. Araki and H. Yamamoto, Solubility of Oxygen in Organic Solvents and Calculation of the Hansen Solubility Parameters of Oxygen, *Ind. Eng. Chem. Res.*, 2014, **53**(49), 19331–19337, DOI: 10.1021/ie502386t.
18 W. Xing, M. Yin, Q. Lv, Y. Hu, C. Liu and J. Zhang, 1 – Oxygen Solubility, Diffusion Coefficient, and Solution Viscosity, In *Rotating Electrode Methods and Oxygen Reduction Electrocatalysts*, ed. W. Xing, G. Yin and J. Zhang, Elsevier, Amsterdam, 2014, pp. 1–31, DOI: 10.1016/B978-0-444-63278-4.00001-X.